

Title	Laser Weldability of Aluminum Alloys(Physics, Processes, Instruments & Measurements)
Author(s)	Katayama, Seiji; Mizutani, Masami
Citation	Transactions of JWRI. 2002, 31(2), p. 147-155
Version Type	VoR
URL	https://doi.org/10.18910/7674
rights	
Note	

Osaka University Knowledge Archive : OUKA

<https://ir.library.osaka-u.ac.jp/>

Osaka University

Laser Weldability of Aluminum Alloys[†]

KATAYAMA Seiji* and MIZUTANI Masami**

Abstract

This study was performed with the objective of producing sound laser weld beads in aluminum alloys. CO₂ and YAG laser weldability of aluminum alloys was investigated in terms of penetration and porosity formation. Deeply penetrated welds were easily formed in alloys with a considerable content of Mg, Li or/and Zn in an inert shielding gas, and deep penetration was obtained in any alloy welded with a CO₂ laser beam in a nitrogen shielding gas. Welding phenomena, keyhole behavior, and the formation mechanism and preventive remedies for bubble formation and porosity were examined by observation through high-speed video cameras and the x-ray transmission imaging system. It was especially revealed that many bubbles were chiefly generated from a keyhole tip, resulting in the formation of porosity. Porosity formation tendency was interpreted in terms of keyhole stability, vapor ejection direction and melt flows depending mainly upon the welding speed. It was also found that a melt flow in vacuum was different from that in general welding at low speeds in Ar or He gas, and consequently no porosity formation was attributed to no bubble generation. The size and number of pores could become smaller and be reduced at low welding speeds under the negative pressure achieved by a newly developed tornado nozzle.

KEY WORDS: (Laser Welding) (Aluminum Alloys) (Weldability) (Porosity) (Penetration) (Bubbles) (Melt Flow)

1. Introduction

Aluminum alloys have been gaining extensive utilization in a variety of constructions and industrial products such as airplanes, ships, tankers, railroads, automobiles and pressure vessels because of weight saving and recycling possibilities, in addition to excellent properties such as relatively high strength-to-weight ratio, good corrosion resistance, high thermal conductivity, good workability, good cryogenic properties, etc. Recently, in the fields of such applications, the necessity for improvement in functions, quality, weight, reliability and productivity has grown, and accordingly the development of welding and joining technologies with higher performance, precision and speed has been required.

Laser welding process, which can offer labor-reduction,

robotization, full automation, and systematization in operational lines, has received great attention as a promising method of achieving high quality, high accuracy, high speed and high productivity in the joining of various constructions and industrial products. Recently, CO₂, YAG, LD and LD-pumped solid-state laser apparatuses as well as their welding applications have been intensively developed. However, several problems may occur during the welding of aluminum alloys under the improper conditions: (1) It is difficult to produce deeply penetrated welds constantly from beginning to end; (2) Surface appearances are not always good due to occurrence of severe spattering; (3) Weld imperfections such as porosity and hot cracking are easily formed in deeply penetrated weld beads, and so on^{1), 2)}. Thereupon, it is necessary to examine the welding phenomena and the

[†] Received on November 20, 2002

* Professor

** Technical Official

Transactions of JWRI is published by Joining and Welding Research Institute of Osaka University, Ibaraki, Osaka 567-0047, Japan

formation mechanisms of welding defects and to develop the preventive remedies for imperfections.

In this study, therefore, penetration characteristics and defect formation conditions of several aluminum alloys were investigated during welding with high-power YAG and CO₂ laser in various shielding gases. In particular, with the objectives of elucidating keyhole-type welding phenomenon and porosity formation mechanisms, keyhole behavior, bubble and pore formation, and melt flows in the molten pool were observed through the microfocused x-ray transmission in-situ imaging system. The gas constituents inside the porosity and the features of pore surfaces were analyzed with the special Q-mass spectroscopic analysis technique, and SEM, EPMA and EDX methods. Furthermore, welding was performed in vacuum or in an inert gas vortex flow using a newly developed "tornado nozzle" for the development of porosity prevention procedures.

2. Materials, X-Ray Transmission In-Situ Imaging System and Experimental Procedure

The materials used were commercially available aluminum alloys, such as 2219, 3003, 5052, 5456, 5083, 6061 and 7075. Penetration was investigated using 6 to 12 mm thick A5083 plate samples with W particles or Sn wires for the observation of melt flows in the molten pool or the puddle geometry during laser welding.

The lasers utilized were continuous wave CO₂ lasers with the maximum power of 3.5, 5.5 or 45 kW and a YAG laser with the maximum power of 4 kW. The laser powers and welding speeds used mainly were 3, 5 and 10 kW, and 10 and 25 mm/s.

A schematic arrangement of the microfocused x-ray in-situ imaging system during CO₂ laser welding is shown in Fig. 1. It consists of a microfocused X-ray tube with the maximum voltage of 160 kV and the maximum current of 1 mA, image-intensifier (I.I.), a high-speed video camera and a worktable. The formation behavior of a keyhole, bubbles and pores during CO₂ or YAG laser welding was observed using this system²⁾⁻⁹⁾.

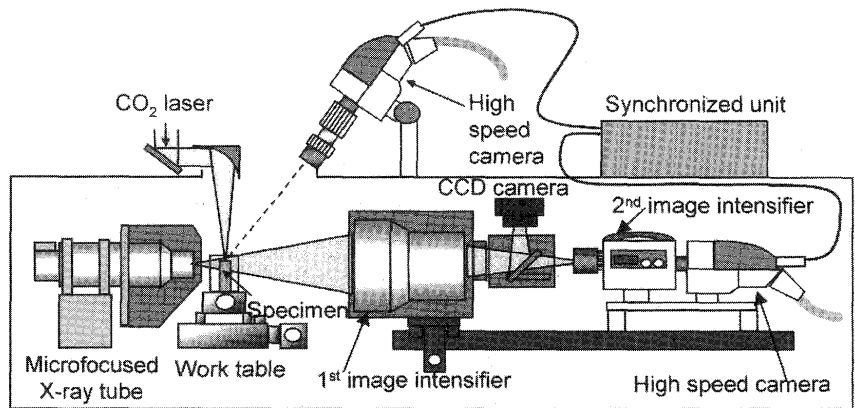


Fig. 1 Schematic arrangement of X-ray transmission imaging system and high-speed video cameras for simultaneous observation of keyhole behavior and porosity formation as well as laser-induced plasma/plume during laser welding.

3. Penetration Characteristics of Laser Welds in Various Aluminum Alloys, and the Effect of Welding Conditions on Penetration

Various alloys, whose surfaces were polished with Emery paper and cleaned with acetone, were subjected to CO₂ laser welding under the same conditions. The penetration depths and widths of the weld beads are comparatively summarized in Fig. 2. The alloys show a different melting tendency depending upon the alloy compositions, and the alloys rated for easier melting and deeper penetration are as follows: 1100, 3003 < 2219 < 6061, 2024 < 7075, 5456, 2090¹⁰⁾.

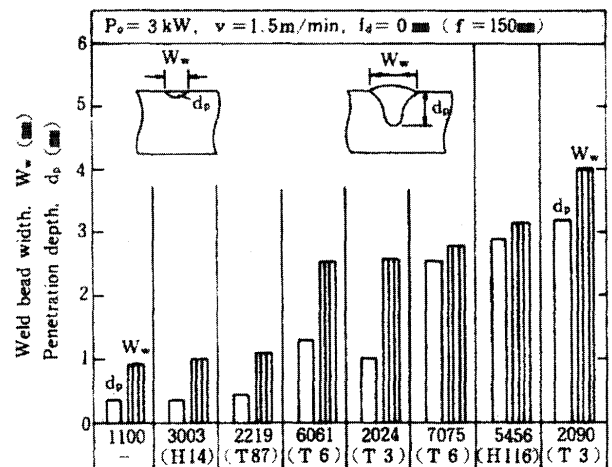


Fig. 2 Comparison of penetration depths and widths of CO₂ laser weld beads in various aluminum alloys.

The effect of a defocused distance on the penetration depth and bead width of various alloy laser welds is indicated in Fig. 3¹¹⁾. The deepest penetration was obtained near the distance of -1 mm, and the penetration became shallower with an increase in the defocused distance. Deeply penetrated welds were produced in 5083, 5182 and 7N01 alloys in the wider ranges of the defocused distance, while the weld penetration depths suddenly became shallow in 5052 and 6061 alloys at longer defocused distances in either plus or minus direction.

From these results, it was confirmed that deep penetration could be easily obtained in the alloys containing relatively high contents of Mg, Zn and Li. Such melting tendency was similarly observed under the other conditions of various laser powers and welding speeds.

Figure 4 exhibits cross sections of A5052 welds produced with CO₂ laser in a variety of coaxial shielding gases¹¹⁾. At the low speed of 25 mm/s, deeper penetration was obtained in He gas than in Ar gas, while at the high speed of 150 mm/s the penetration was deeper in Ar gas and a heat-conduction type of shallow welds were produced in the gases containing He of 50% or more. This melting tendency is attributed to the difference in the formation of laser-induced Ar gas plasma and no formation of He gas plasma. Namely, the gas plasma acts as an absorber of laser energy and a heater of the A5052 plate surface at high and low welding speeds, respectively. Moreover, a keyhole type of deep penetration can be obtained at any welding speed in N₂ gas. It is judged in CO₂ laser welding that N₂ gas is beneficial for a reduction in laser-reflection and the enhancement of melting because of the formation of AlN nitride film on the plate surface. In YAG laser welding, however, the effect of N₂ gas is not present because AlN nitride films are not formed on the molten pool surface¹²⁾. Welding phenomena in the different shielding gases will be investigated in more details in the next section. In 5083 and 5182 alloys, which were judged to be easier to melt deep penetration welds could be easily obtained in both CO₂ and YAG laser welding.

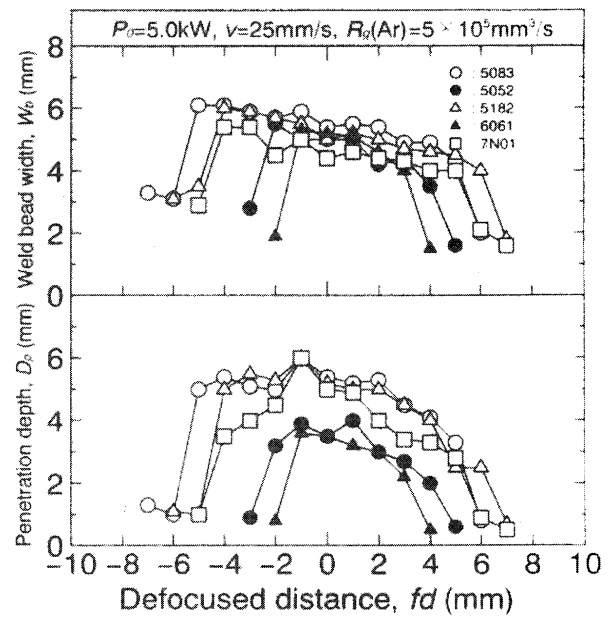


Fig. 3 Effect of defocused distance on penetration depth and bead width of CO₂ laser weld fusion zones in different aluminum alloys.

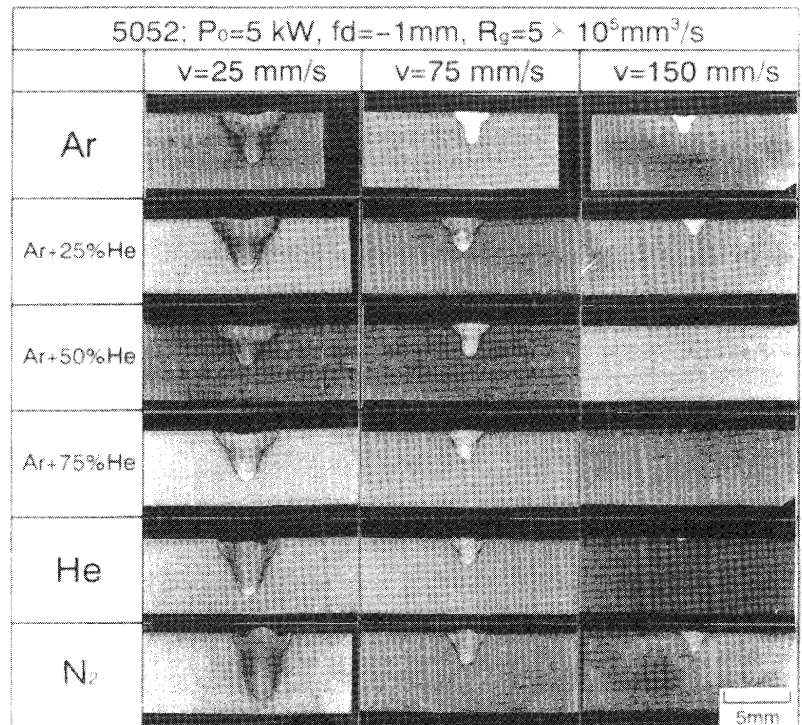


Fig. 4 Summary of cross sections of laser weld fusion zones in A5052 alloy, showing effect of shielding gas on penetration.

4. Elucidation of Laser Welding Phenomena and Porosity Formation Mechanism

4.1 Penetration of laser weld, and plasma/plume behavior

CO₂ laser bead-on-plate welding was carried out in He, Ar and N₂ coaxial shielding gases. The cross-sections of laser welds and laser-induced plasma/plumes observed are shown in Figs. 5 and 6²⁾. The penetration depths of the welds are shallower in the order of He, N₂ and Ar. Porosity is also present in deeply penetrating welds. In the case of CO₂ laser welding, a metallic plume only is seen in He gas, while gas plasmas in addition to metallic plumes are observed above the keyhole in Ar and N₂ gases. The metallic plumes moved around or toward the front and the rear at low welding speeds, and the ejection or eruption of the plume approached the laser irradiation direction with an increase in the speed. Moreover, in the case of powers of 10 kW or more, when Ar or N₂ plasma-control gas was aimed from the upper oblique direction,

its gas plasma was periodically generated and lifted off toward the laser irradiation direction^{6),13)}, and a keyhole behaved in the way similar to pulse-modulated laser welding⁶⁾. In Ar, a big gas plasma was formed at shorter intervals, resulting in the production of much shallower welds. It is therefore judged that the effect of a gas plasma on the weld geometry and penetration depth is quite large. The effects of the plasma are interpreted in terms of absorption of the laser beam due to the inverse bremsstrahlung, defocusing due to a plasma lens formed by the refractive index distribution, and deflection due to an off-axis inclination of the plasma lens, and so on^{14),15)}, but it should be investigated further in the future.

In high-power YAG laser welding, brilliant plumes of metallic vapors were ejected from the keyhole but no gas plasmas were detected in He, Ar and N₂ shielding gases. The penetration depths of their welds are almost equal and the effect of shielding gas is small. This result is different from that of CO₂ laser welding, which signifies a great effect of laser wavelength on the plasma formation and penetration.

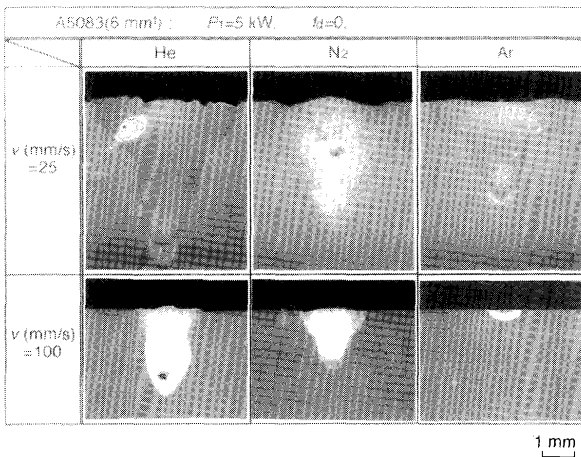


Fig. 5 Cross sections of CO₂ laser weld beads of A5083 produced in He and N₂ shielding gas, showing the effect of gas kind on penetration.

4.2 Keyhole behavior and bubble and porosity formation during laser welding

Porosity was formed in deeply penetrating welds in aluminum alloys produced with high-power lasers, as already shown in Fig. 5. Bubble and porosity formation situations during high-power CO₂ laser welding were observed through microfocused x-ray transmission imaging system. Figure 7

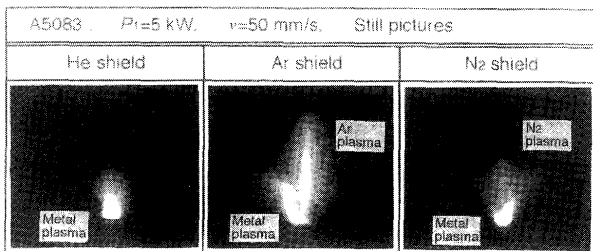


Fig. 6 Plasma plume during CO₂ laser welding in He, Ar and N₂ shielding gas, showing difference of laser-induced plasma.

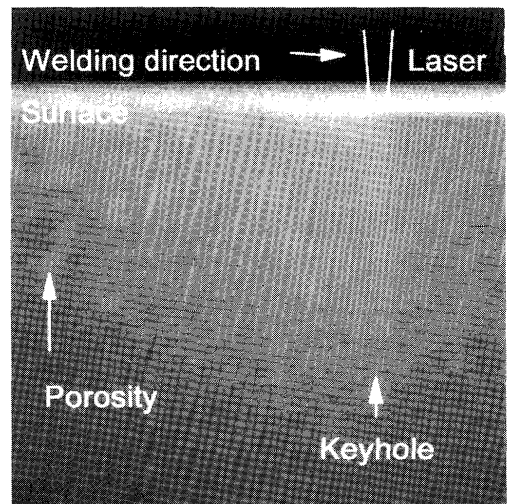


Fig. 7 X-ray transmission observation photo during CO₂ laser welding of A5083 alloy at P₁=10 kW, v=25 mm/s, and f_d=0 mm in He gas, showing keyhole, bubbles and porosity formation.

shows an example of an observation during laser welding of A5083 alloy⁹⁾. It was observed that bubbles were generated in the molten pool from the vicinity of the keyhole tip and thereafter moved toward the rear-upper part of the solidifying front. The movement of a floating bubble was measured, and

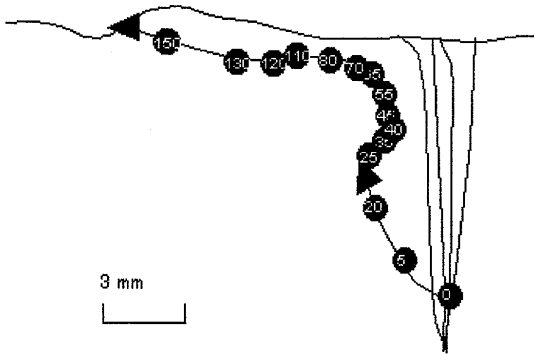
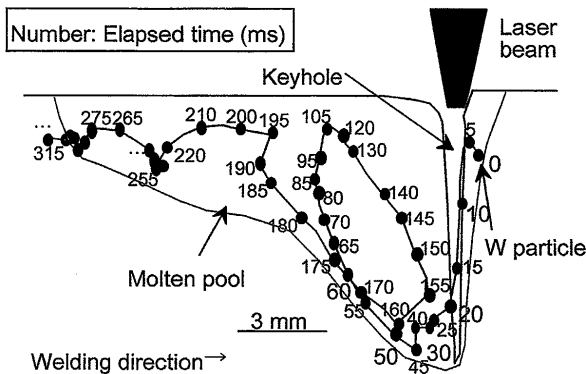
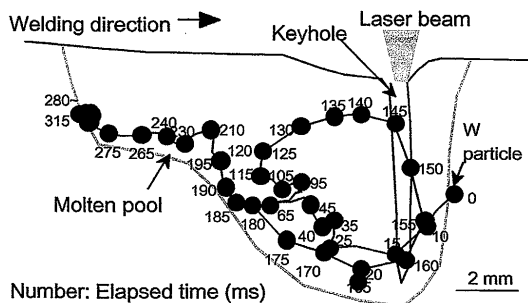


Fig. 8 Measured movement of bubble during CO₂ laser welding of A5083 alloy.



(a) CO₂ laser (10 kW, 25 mm/s)



(b) YAG laser (3.5 kW, 10 mm/s)

Fig. 9 Measured movement of W particle during CO₂ and YAG laser welding of A5083.

an example is indicated in Fig. 8. Pores were formed at a variety of locations by the capture of floating bubbles in A5083 alloy welds. It was observed that some bubbles disappeared from the molten surface or into a keyhole during welding. Therefore, such disappearance of bubbles during welding of A5083 alloy resulted in a decrease in porosity in the case of low welding speeds.

As the welding speed increased, a keyhole became narrower and shallower, bubbles became smaller, and consequently both the size and the number of pores decreased, although these bubbles did not reach the surface of the molten pool⁹⁾. Therefore, the formation ratio or volume of porosity is high or large at a certain welding speed. The formation situations of bubbles and porosity were similar in YAG and CO₂ laser welding.

Melt flows were measured by observing the movement of W particles. The results during CO₂ and YAG laser welding of A5083 alloy are shown in Fig. 9 (a) and (b)⁹⁾. W particles were heavy, but nevertheless they moved from the bottom front toward the upper rear near the solidifying front. The movement was similar to that of a bubble and was fastest near the bottom of the molten puddle. From these results, it is judged that a bubble is chiefly carried along melt flows but not by its buoyancy.

The insides of pores in laser weld metals were observed with SEM. Figure 10 shows the results of SEM observation and EDX analyses of Al, Mg and O on the pore surface in YAG laser weld metal of A5083 alloy. Mg and O are enriched in white films on the surface. It is considered that the film is an

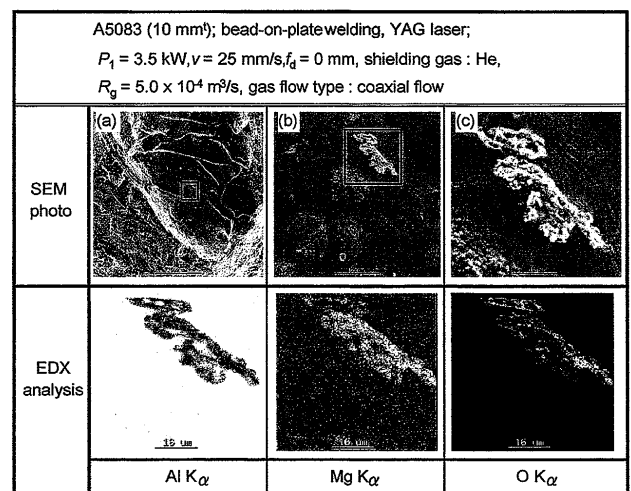


Fig. 10 SEM photo and EDX analysis results, showing formation of oxide.

Laser Weldability of Aluminum Alloys

oxide of the $MgAl_2O_4$ type and there are many Mg-enriched vapors in the original bubble. The same results were obtained in CO_2 laser welds.

The gas constituents inside the pores in laser weld beads were analyzed. The results of porosity in A5083 alloy welded with CO_2 and YAG laser under the various conditions are summarized in **Table 1**. It is understood that shielding gas was mainly contained in the pores, although hydrogen gas and nitrogen gas from the atmosphere were also detected. Oxygen must reduce by combining with metallic vapors. Hydrogen

content also increased with the elapse of time. It is therefore deduced that bubbles leading to the porosity are formed by intense evaporation at the keyhole front near the bottom of the molten pool and a shielding gas in addition to metallic vapors is entrained and involved into the keyhole and bubbles.

Keyhole behavior, bubble and porosity formation situation, melt flows in the molten pool during laser welding at various speeds were observed through X-ray transmission method. Based upon the observation results, welding phenomena are schematically illustrated in **Fig. 11**. At low welding speeds, a keyhole is liable to collapse, a laser beam is shot on the liquid wall of the collapsed keyhole, and consequently the downward melt flow along the keyhole wall is induced by the recoil pressure of evaporation. Moreover, intense evaporation takes place at the front wall of the keyhole, and thereby many bubbles are generated from the keyhole tip. As the welding speed increases, vapors generated from the keyhole wall are more readily ejected upwards from the keyhole mouth or inlet. As a result, an upward melt flow is induced near the keyhole inlet, and the downward flow near the keyhole tip is reduced. A bubble moves in a short distance, and the formation location of porosity is limited near the bottom.

Table 1 Q-mass analysis results of gases (vol%) inside pores in laser weld fusion zone of A5083 alloy.

Laser kind (shielding gas; power)	Ar	He	H ₂	Others
CO_2 laser (Ar; 5 kW)	41	-	59	-
CO_2 laser (He; 10 kW)	0.6	95.9	3.3	0.2 N ₂
CO_2 laser (He; 10 kW)	0.6	86.8	12.6	-
YAG laser (He; 3 kW)	-	99.2	0.6	0.2 N ₂

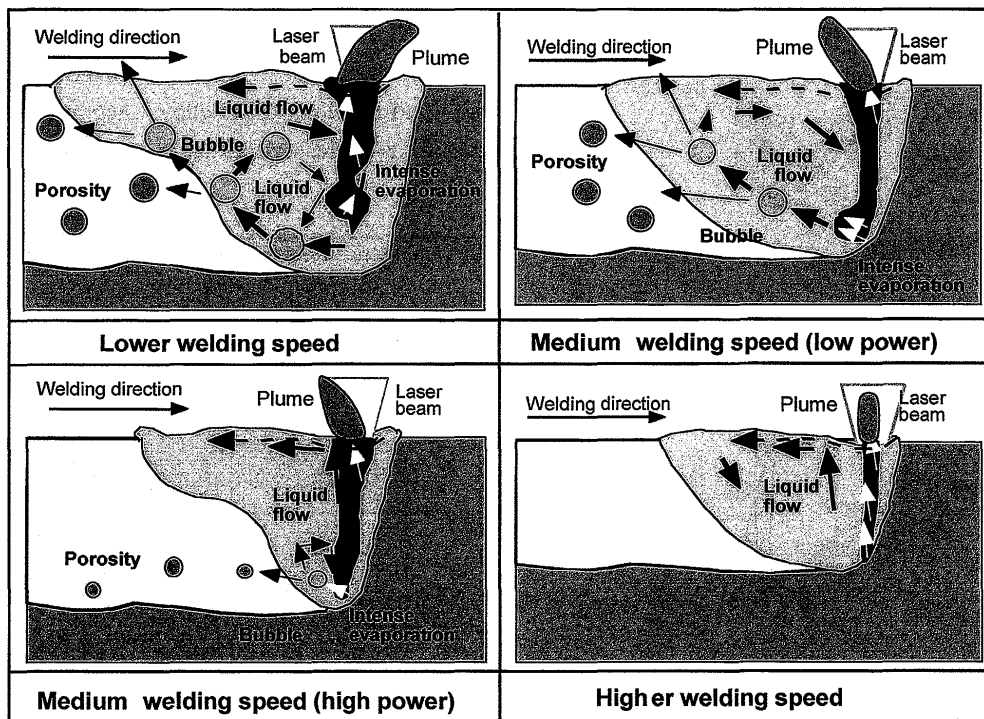


Fig. 11 Schematic illustration showing effects of evaporation direction and fluid flows on bubble formation and movement during CW laser welding at various speeds.

The formation of bubbles is suppressed at higher welding speeds. The strong upward stream can prevent shielding gas from entering into the keyhole and also induce an upward melt flow along the keyhole wall (which is the reverse of laser welding at low speeds), resulting in the prevention of the bubble generation leading to porosity formation.

5. Investigation of Porosity Reduction Methods during Laser Welding

5.1 Several Methods for Porosity Reduction or Suppression

In partial-penetration laser welding at low speeds, many bubbles were generated from a keyhole tip and result in the formation of porosity. Therefore, the feasibility of porosity prevention was investigated by observing x-ray transmission images during full penetration laser welding. As a result, it was confirmed that no bubbles were generated when a keyhole was fully penetrated. The phenomenon of a bubble escaping from the bottom of the molten pool has not been observed.

The generation of bubbles from a keyhole tip was attributed to easy collapse of the keyhole due to a long interaction time between an incident laser and a keyhole wall. Thereafter, bead-on-plate welding with a pulse-modulated laser beam was performed and keyhole behavior was observed through x-ray transmission images. It was consequently confirmed that bubble generation could be prevented by a

proper combination of the pulse width and the repetition rate, leading to the suppression of porosity.

Moreover, other several procedures for reducing porosity were examined. A shielding gas was included into a pore. Therefore, vacuum welding and the welding with a tornado nozzle were conducted to elucidate a feasibility of porosity suppression and the effective reduction mechanism. The results will be discussed in the following sections.

5.2 Laser welding phenomena in vacuum and porosity reduction mechanism

YAG laser welding was done with coaxial shielding gas flow or under low pressure. The cross sections and x-ray inspection results of laser welds in A5083 alloy and x-ray transmission images during welding are shown in Fig. 12⁸⁾. It was confirmed that the penetration depth was deeper and the amount of porosity was decreased with a decrease in the chamber pressure. No porosity was present in the weld made under the conditions of low pressure or high vacuum. It was observed that, under the low pressure or high vacuum, no bubbles, leading to no porosity, were generated although the keyhole tip swelled or grew bigger. Moreover, it was revealed that the upward melt flows along the keyhole wall, which were quite different from those during general laser welding at low speeds, were prevailing under the high vacuum conditions⁸⁾.

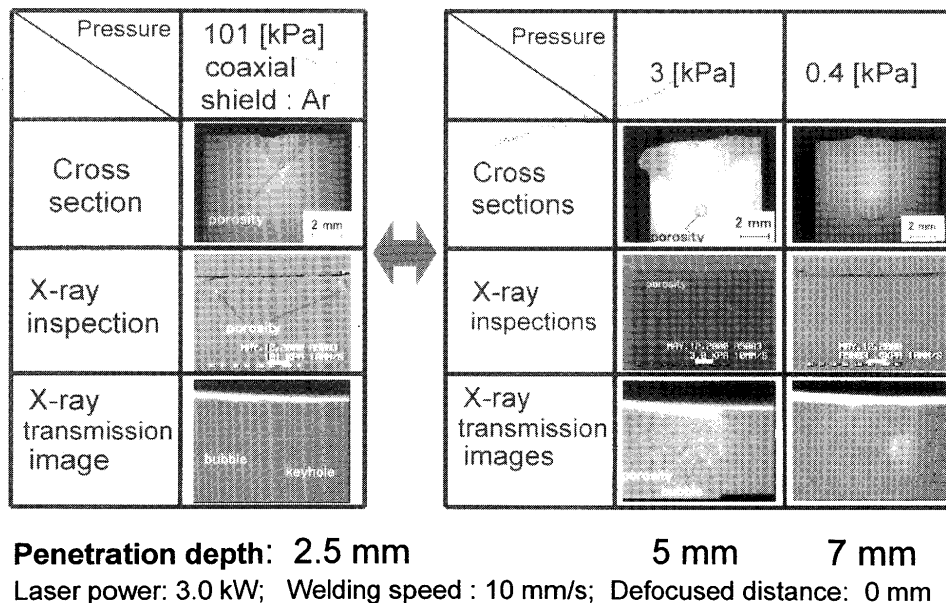


Fig. 12 Comparison of cross sections, X-ray inspection results and X-ray imaging photos of A5083 alloy welded with YAG laser under various pressure levels.

5.3 Effect of vortex gas flow on porosity reduction

A newly devised tornado nozzle for vortex gas flows was produced, and the gas pressure was measured. The results using Ar and He gas are indicated in Fig. 13¹⁶⁾. It is confirmed that a negative pressure can be achieved near the nozzle central axis. The degree of the negative pressure is higher in a higher density of Ar gas than in a lower density of He gas at the same flow rate.

CO₂ laser welding was performed using the tornado

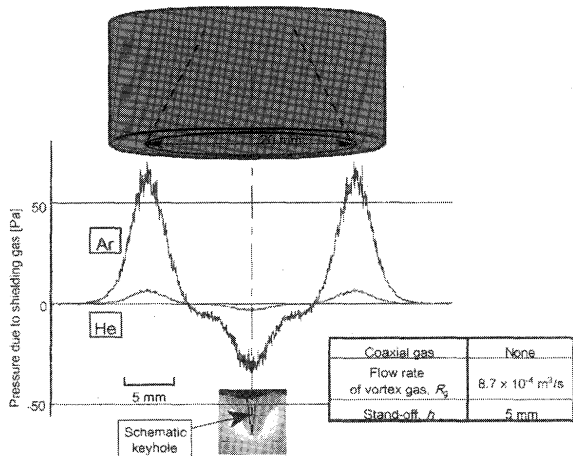


Fig. 13 Comparison of gas pressure distribution on specimen surface in Ar and He gas.

nozzle. Examples of the results are shown in Fig. 14¹⁶⁾. As the degree of the negative gas pressure increases, it is found that the size and amount of pores decrease. It was confirmed that the effect of the negative pressure with the tornado nozzle was greater at the lower speed in both CO₂ and YAG laser welding.

6. Conclusions

A variety of aluminum alloys were subjected to CO₂ and YAG laser welding under various conditions. Also, keyhole behavior, bubble and porosity formation, and melt flows in the molten pool were observed using a high-speed video camera and the x-ray transmission imaging system. The following results are obtained:

- (1) The effects of alloy composition and shielding gas on the penetration were confirmed; Mg, Zn and Li, and N₂ gas were effective to promote deeper penetration.
- (2) It was found that a laser-induced gas plasma was formed during CO₂ laser welding in Ar or N₂ gas.
- (3) Bubbles were generated from a keyhole tip, and floated along the melt flows in the molten pool. When some bubbles are captured or trapped by the solidifying front, they cause porosity, whose location depends upon the captured position.
- (4) Melt flows are affected by welding conditions, especially welding speed.

A5083 (10 mm ^l); bead-on-plate welding with CO ₂ laser; P ₁ = 5.0 kW, f _q = 0 mm (f = 254 mm), h = 10 mm, shielding gas : He							
Gas flow type	Coaxial flow [m ³ /s]		Vortex flow [m ³ /s]				
Coaxial	5.0 × 10 ⁻⁴		6.7 × 10 ⁻⁴		3.3 × 10 ⁻⁴		
Vortex	—		6.7 × 10 ⁻⁴		6.7 × 10 ⁻⁴		
Typical gas pressure distribution							
12.5							
25							
50							
Welding speed [mm/s]	Cross section	X-ray inspection	Cross section	X-ray inspection	Cross section	X-ray inspection	

Fig. 14 Effect of vortex gas flow on weld penetration and porosity formation in weld metals of A5083 alloy produced with CO₂ laser at speeds of 12.5, 25 and 50 mm/s.

- (5) The amount of porosity decreased with an increase in the welding speed at high speeds. In this case, melt flow occurred upward along the keyhole wall, which was considered to suppress the formation of porosity.
- (6) It was confirmed that full-penetration keyhole laser welding, pulse-modulated laser welding, high vacuum (low pressure) laser welding, and negative pressure welding with a tornado gas nozzle were effective in reducing porosity.

Acknowledgements

This study was executed partly under the NEDO photon project and fundamental researches (C) (No. 09650788 and 11650740: Representative researcher: KATAYAMA Seiji) and the authorities related should be appreciated. The authors also heartily thank Dr. MATSUNAWA Akira, Professor Emeritus of Osaka University, Dr. YOKOYA Shin-ichiro, Professor of Nippon Institute of Technology, as well as Dr. KIM Jong-do, Dr. SETO Naoki, Mr. YOSHIDA Daisuke, Mr. KOBAYASHI Yoshihiro, former graduate students of Osaka University, for their cooperative experimental work.

References

- 1) S. Katayama: "Laser Welding of Aluminum Alloys -Present State and Problems-", Proc. of 26th Laser Materials Processing Conference Sponsored by Japan Laser Processing Society (JLPS), 26 (1991, 7), pp.145-158. (in Japanese)
- 2) S. Katayama and A. Matsunawa: "Laser Weldability of Aluminum Alloys", Proc. of 43rd Laser Materials Processing Conference Sponsored by JLPS, 43 (1998, 3), pp.33-52. (in Japanese)
- 3) S. Katayama, N. Seto, J.D. Kim and A. Matsunawa: "Formation Mechanism and Reduction Method of Porosity in Laser Welding of Stainless Steel", Proc. ICALEO '97, Vol.83-Section G, (1997), pp. 83-92.
- 4) S. Katayama and A. Matsunawa: "Formation Mechanism and Prevention of Defects in Laser Welding of Aluminium Alloys", Proc. CISFFEL 6, Vol.1 (1998), pp.233-240.
- 5) S. Katayama, N. Seto, J.D. Kim and A. Matsunawa: "Formation Mechanism and Suppression Procedure of Porosity in High Power Laser Welding of Aluminum Alloys", Proc. ICALEO '98, Vol.85-Section C, (1998), pp. 24-33.
- 6) N. Seto, S. Katayama and A. Matsunawa: "High-Speed Simultaneous Observation of Plasma and Keyhole Behavior during High Power CO₂ Laser Welding: Effect of Shielding Gas on Porosity Formation", J. of Laser Applications, 12-6 (2000), pp. 245-250.
- 7) S. Katayama, N. Seto, M. Mizutani and A. Matsunawa: "Formation Mechanism of Porosity in High Power YAG Laser Welding", Proc. ICALEO 2000, Vol.89-Section C, (2000), pp.16-25.
- 8) S. Katayama, Y. Kobayashi, M. Mizutani and A. Matsunawa: "Effect of Vacuum on Penetration and Defects in Laser Welding", J. of Laser Applications, 13-5 (2001), pp.187-192.
- 9) S. Katayama and A. Matsunawa: "Dynamic Behaviour of Keyhole and Molten Pool in High Power Laser Welding", Proc. of 7 International Aachen Welding Conference -High Productivity Joining Processes, Fundamentals, Applications, Equipment-, ed. by U. Dilthey, Aachen, Germany, Vol. 1 (2001, 5), pp. 133-143
- 10) S. Katayama and C. D. Lundin: "Laser Welding of Commercial Aluminium Alloys (Report II)", J. of Light Metal Welding & Construction, 29-8 (1991), pp. 349-360. (in Japanese)
- 11) A. Matsunawa, K. Kojima and S. Katayama: "CO₂ Laser Weldability of Aluminium Alloys (Report I)", J. of Light Metal Welding & Construction, 35-10 (1997), pp. 461-472. (in Japanese); Welding International, 12-7 (1998), pp.519-528.
- 12) S. Katayama, D. Yoshida and A. Matsunawa: "Assessment of YAG and CO₂ Laser Weldability in Nitrogen Shielding Gas", Proc. ICALEO 2000, Vol.89 (2000), Section C, pp.42-51.
- 13) T. Ishide, S. Shono, T. Ohmae, H. Yoshida and A. Shinmi: "Fundamental Study of Laser Plasma Reduction Method in High Power CO₂ Laser Welding", Proc. LAMP'87, Osaka, (1987), pp. 187-191.
- 14) I. Miyamoto and H. Maruo: "Spatial and Temporal Characteristics of Laser-Induced Plasma in CO₂ Laser Welding", Proc. of LAMP '92, Nagaoka, (1992), pp.311-316.
- 15) H. Schittenhelm, J. Muller, P. Berger and H. Hugel: "Investigation on CW CO₂-Laser Induced Welding Plasmas Using Differential Interferometry", Proc. ICALEO '99, Vol.87-Section E, (1999), pp. 195-204.
- 16) S. Katayama, D. Yoshida, S. Yokoya and A. Matsunawa: "Development of Tornado Nozzle for Reduction in Porosity during Laser Welding of Aluminum Alloy", Congress Proc. of ICALEO 2001 (Laser Materials Processing Conference), (2001), Session C: Welding, 1701 (CD).